Prediction of Pressure Fluctuations Beneath Hydraulic Jump Using Neural Networks

M.Sc. Thesis Report

in

Civil Engineering Department
University of Gaziantep

Supervisor:

Assoc. Prof. Dr. Mustafa GÜNAL

by

Ömer Faruk ALTAN

June 2007

ABSTRACT

MODELING OF PRESSURE FLUCTUATION

BENEATH HYDRAULIC JUMP

ALTAN, Ömer Faruk

M.Sc. in Civil Engineering

Supervisor : Assoc. Prof. Dr. Mustafa GÜNAL

June 2007, 60 pages

Various types of hydraulic jump occurring on horizontal and sloping channels have been analyzed experimentally and theoretically, and the results are available in the literature. In this study, Artificial Neural Network (ANN) models were developed to simulate the mean pressure fluctuations beneath hydraulic jump occurring on horizontal stilling basins. Multilayers feed forward neural network with back propagation learning algorithm is used to model the pressure fluctuations beneath hydraulic jump. Explicit formulations of mean pressure fluctuation and dimensionless pressure fluctuation parameter in terms of the most contributing characteristics of hydraulic jump occurring on stilling basins are presented. The proposed neural network models are compared with nonlinear regression models that were developed using considered physical parameters. The results of the neural network modelling are found to be superior over the regression models and are in good agreement with the experimental results due to relatively small values of error (mean absolute percentage error).

Keywords: Neural networks, pressure fluctuations, hydraulic jump, stilling basin, explicit neural networks formulation, regression analysis.

ÖZ

HİDROLİK SIÇRAMA ALTINDA OLUŞAN BASINÇ ÇALKANTILARININ MODELLEMESİ

ALTAN, Ömer Faruk
Yüksek Lisans Tezi, İnşaat Müh. Bölümü
Tez Yöneticisi : Doç. Dr. Mustafa GÜNAL
Haziran 2007, 60 sayfa

Yatay ve eğimli kanallarda oluşan hidrolik sıçramanın çeşitli tipleri deneysel ve teorik olarak çalışılmıştır ve bu çalışmaların sonuçları literatürde mevcuttur. Bu çalışmada, yatay enerji kırma havuzlarında meydana gelen hidrolik sıçrama altında oluşan ortalama basınç çalkantılarının Yapay Sinir Ağları (YSA) ile modellemeleri gerçekleştirilmiştir. Çok katmalı ileri beslemeli sinir ağı ve geri beslemeli öğrenme algoritması kullanılarak bu tip hidrolik sıçrama altında oluşan ortalama basınç çalkantıları modellenmiştir. Yatay enerji kırma havuzlarında meydana gelen hidrolik sıçramayı en çok etkileyen parametreler kullanılarak, ortalama basınç ve boyutsuz basınç çalkantısı parametresinin açık formülasyonları sunulmuştur. Önerilen sinir ağı modelleri, aynı fiziksel parametreler kullanılarak elde edilen lineer olmayan regresyon modelleriyle karşılaştırılmıştır. Sinir ağı modellerinin sonuçlarının, lineer olmayan regresyon modellerine göre çok daha iyi olduğıu gözlemlenmiştir, ve deneysel sonuçlarla da nisbeten küçük hatalar (ortalama salt yüzde hata) ile birlikte iyi uyum içinde olduğu gözlemlenmiştir.

Anahtar kelimeler: Sinir ağları, basınç çalkantıları, hidrolik sıçrama, enerji kırma havuzu, açık sinir ağı formülasonu, regresyon analizi.

ACKNOWLEDGEMENTS

Firstly, I would like to express my deep gratitude to my supervisor, Assoc. Prof. Dr. Mustafa GÜNAL, for his invaluable guidance, continous advice and providing continous encouragement. He provided me stimulation and constructive criticism throughout the development of this research.

Sincere thanks to Reserach Assistant Aytaç GÜVEN for his guidance and constructive discussion on this thesis. He gave me invaluable advices while dealing with problems during this study.

Lastly, but by no means least, I would like to thank to my family for their continous encouragement and stimulation during the period of this study.

TABLE OF CONTENTS

LIST OF FIGURES

LIST OF TABLES

List of symbols

C_p	non-dimensional mean pressure parameter
$C_p^{'}$	non-dimensional pressure fluctuation parameter
L_s:	the distance from the toe of the jump to the point where the slope joins the channel bed
p	instantaneous pressure
$\overline{p}$	mean part of pressure
$p^{'}$	fluctuating part of pressure
pi	regression model parameters
$\sqrt{\overline{p'^2}}$	root mean square value of pressure fluctuation
U_i	sum up of weighted inputs
y_1	gate opening
u_1:	upstream velocity of water issuing from the gate
y_t:	tail water depth
x:	the distance from the gate to the pressure fluctuation measurement point
ϕ:	inclination angle of the sloping part of channel in degrees
g:	gravitational acceleration
ρ_w:	the density of water.

CHAPTER 1

INTRODUCTION

Hydraulic jump occurs when the upstream flow is supercritical (F>1). To have a jump, there must be a flow impediment downstream. The downstream impediment could be a weir, a bridge abutment, a dam, or simply channel friction. Water depth increases during a hydraulic jump and energy is dissipated as turbulence. Often, engineers will purposely install impediments in channels in order to force jumps to occur. Mixing of coagulant chemicals in water treatment plants is often aided by hydraulic jumps. Concrete blocks may be installed in a channel downstream of a spillway in order to force a jump to occur thereby reducing the velocity and energy of the water. Flow will go from supercritical (F>1) to subcritical (F<1) over a jump.

Hydraulic jump is a rapidly varied transition from supercritical to sub-critical flow through which energy is dissipated due to generation of large-scale turbulence. The turbulence intensity is responsible for conversation of mechanical energy to heat. This phenomenon is widely used as an efficient energy dissipater in spillway stilling basins to dissipate the high energy contained in water passing down the spillway chute. This process is associated with low frequency dynamic pressures acting on the floor and side walls of stilling basins. These dynamic pressures may cause severe damages to the structures such as, lifting up the whole floor slabs, fatigue of materials, or large instantaneous depression which could produce intermittent cavitations. Major damages

due to pressure fluctuations have been reported in several spillway stilling basins. The magnitude and extend of these fluctuating pressures are strongly depend on the geometry of stilling basin, incoming flow conditions and Froude number. However, there is still a lack of information on the effect of these macro turbulent pressure fluctuations and their quantitative values.

Numerical modelling has been applied to describe the physical processes occurring in the aquatic environment for some 30 years. Physical modelling requires expensive instruments, test rigs and skilled workers, as well as being highly time-consuming and difficult in many cases to repeat with the same experimental conditions with high precision. Therefore, it calls for use of numerical and mathematical modelling that is well established and widely accepted technique. Numerical modelling is applied in many areas of hydraulic engineering like sediment transport, two-phase flows, turbulent flows, etc. However, despite their many successes, a wider application of these models is restrained by their heavy demand in computing capacity and time. It has been obtained that for applications like real-time and near-real-time control, the demand on computing time and resources are of the huge magnitudes that are sometimes far from acceptable. Recent developments in sub-symbolic techniques (Artificial Neural Networks, Classifier Systems, Genetic Programming, Fuzzy Logic, etc.) have made them more potential in simulating physical processes, based on measured data.

ANN is recently widely used technique in prediction of hydraulic data. An important advantage of ANNs compared to classical stochastic models is that they do not require variables to be stationary and normally distributed. Furthermore, ANNs are relatively stable with respect to noise in data and have a good generalization potential to represent input-output relationships.

CHAPTER 2

LITERATURE SURVEY

Over the years, several aspects of hydraulic jump forming in horizontal and sloping channels have been investigated. In an open channel, if the downstream depth is greater than the downstream sequent depth, the jump moves upstream to submerge the incoming flow. Such a jump is called a submerged hydraulic jump. The hydraulic jump forming on the stilling basin is a free hydraulic jump if it forms at the foot of the spillway (see Figure 2.1). Usually the jump is enclosed within a stilling basin. On the other hand, if the downstream depth of the flow in the stilling basin is greater than the sequent depth, the hydraulic jump moves towards the spillway with its toe positioned on the spillway. Such a jump is called a B-jump and a B-jump may be considered to belong to the class of submerged jumps with the entering flow at an angle to the bed of the channel. Mean flow characteristics of B-jump were investigated in detail by Hager (1989), and Ohtsu and Yasuda (1990, 1991). These studies relate to the mean velocity measurements, roller length and length of the jump.

Rouse et. al. (1959) studied the intensity of turbulence in hydraulic jump by means of air model. In 1961, Elder performed experimental investigations on model-prototype correlation of pressure fluctuations. Bowers et. al. (1964) reported some information of the damage caused by pressure fluctuations in hydraulic jump to the Karnafuli spillway. Early studies on pressure fluctuations in classical hydraulic jumps were due to Vasiliev and

Bukreyev (1967) concerning the statistical characteristics of turbulent pressures under hydraulic jump. Schiebe and Bowers (1971) studied the statistical characteristics of pressure fluctuations under hydraulic jumps. Leuthesser and Kartha (1972) showed the effect of inflow development on the magnitude of fluctuations using the measurements of velocity fluctuations provided by hot film anemometer. Abdul Khader and Elango (1974) studied the statistical characteristics of fluctuating pressure under hydraulic jumps with froude numbers of 4.7, 5.9, and 6.6 Lopardo et. al. (1982) showed that severe pressure fluctuations may increase the cavitation risk. Akbari et. al. (1982) investigated the turbulence pressure characteristics of the free and forced hydraulic jumps.

Bowers and Toso (1987) presented their results of the model studies of spillway damage for Karnafuli dam. They recommended that if hydraulic jump forms far upstream on the chute, the outlets of drain system and the floor slabs of the chute may subject to high pressure fluctuations in hydraulic jump. Rinaldo, A. and Fiorotto, V. (1993) showed the numerical value of the dimensionless parameter $C_p^{'}$ of fluctuating pressures is sufficiently representative for the instantaneous actions generated by the macro turbulence in the hydraulic jump.

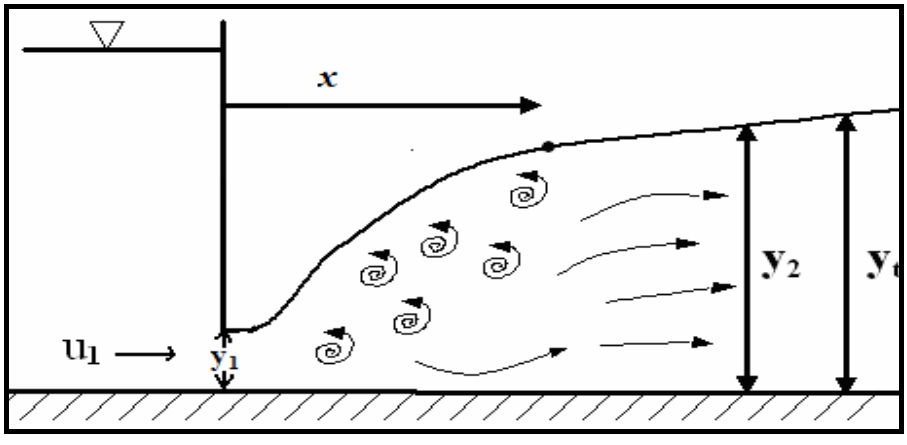

Fig. 2.1. Sketch of hydraulic jump on stilling basin.

Abdul Khader and Elongo (1974), and Lopardo and Henning (1985), Toso and Bowers (1988) and Fattor et al. (2001) studied statistical properties of fluctuating pressures beneath hydraulic jump formed downstream of spillway. On the other hand, Vasiliev and Bukreyev (1967), Narasimhan and Bhargava (1976), Narayanan (1978), and Lopardo et al. (2004) measured intensity of fluctuating pressures beneath submerged and free jumps downstream of sluice gate in the horizontal channel. Clearly these two sets of experiments with respect to hydraulic jumps, one downstream of spillway and the other downstream of sluice gate, are different with respect to the upstream conditions. It is well known that different upstream conditions such as the mean velocity distribution and intensity of turbulence have strong influence on the magnitude of pressure fluctuations and mean flow properties. It is worth noting that the investigations with the jump downstream of spillway do not agree even among themselves. Abdul Khader and Elongo (1974) explained that the large intensity obtained by them is the result of large turbulence level and the upstream velocity profile. The experimental results concerning intensity of pressure fluctuations of Narasimhan and Bhargava (1976) and Narayanan (1978) with the hydraulic jump downstream of sluice gate collapse on to a single curve.

There is another important aspect relating to pressure fluctuations which is of interest to designers of stilling basin. It is well known that the pressure fluctuations can be potentially destructive because they can cause failure due to fatigue, structural vibrations, lifting of whole slabs or they can induce cavitation due to large instantaneous depressions that can lead to damage of material. Bowers et al. (1964) reported some information of the damages caused by pressure fluctuations in hydraulic jump to the Karnafuli spillway. Fattor et al. (2001) studied the destructive action of macro turbulent flows induced by hydraulic jumps in stilling basins with particular focus on cavitation

inception and cavitation damages by severe pressure fluctuations in relatively low velocity flows.

Gunal (1996) carried out experiments for measuring pressure fluctuations for B-Jumps. Experiments were carried out in a flume of rectangular section 0.91 m wide and 3.20 m long, having glass sides. Fluctuating pressure measurements were carried out for three different slopes of $\phi = 10^0, 20^0$ and 30^0. The jet issuing through the sluice opening converges to form a vena contracta with a constant coefficient of 0.93-0.96. Experiments were carried out for three different Froude numbers F_1 at the vena contracta. In order to see the relation between Froude numbers and the intensity of pressure fluctuations for each slope, the hydraulic jump was formed at four different positions in the channel. The position of the jump L_s was measured from the channel junction to the toe of the jump. Further details of this experimental study can be found in Gunal (1996).

CHAPTER 3

NUMERICAL AND DIMENSIONAL ANALYSIS OF PRESSURE FLUCTUATION BENEATH HYDRAULIC JUMP

3.1 Numerical Background

The instantaneous values of the pressure p are separated into mean $\overline{p}$ and fluctuating quantities p' as:

$$p = \overline{p} + p' \tag{3.1}$$

In Equation 3.1, the mean pressure $\overline{p}$ is expressed non-dimensionally as C_p and it is defined as follows:

$$C_p = \frac{\overline{p}}{(\frac{1}{2}\rho u_1^2)} \tag{3.2}$$

In Equation 3.1, the measures of the intensity of pressure fluctuations is their root mean square (r.m.s.) value of $\sqrt{\overline{p'^2}}$, in which p' is the fluctuating part of the pressure over its mean value r.m.s. value of pressure fluctuations $\sqrt{\overline{p'^2}}$ is expressed non-dimensionally using the dynamic pressure of the incoming flow as:

$$C_p^{'} = \frac{\sqrt{\overline{p'^2}}}{(\frac{1}{2}\rho u_1^2)} \tag{3.3}$$

The numerical value of dimensionless parameter $C_p^{'}$ of fluctuating pressures is sufficiently representative for the instantaneous actions generated by the macro turbulence in hydraulic jump (Lopardo et al. 1999). This parameter is important for assessing the effect of the uplift of bottom slabs especially for the tendency to cavitation by pressure pulses.

3.2 Dimensional Analysis

Dimensional analysis is a method for reducing the number and complexity of experimental variables which affect a given physical phenomenon, using a sort of compacting technique. If a phenomenon depends upon n dimensional variables, dimensional analysis will reduce the problem to only k dimensionless variables, where the reduction $n - k = 1, 2, 3$, or 4, depending upon the problem complexity. Generally $n - k$ equals the number of different dimensions which govern the problem. In fluid mechanics, the three basic dimensions are usually taken, the dimension of mass (M), the dimension of length (L), the dimension of time (T) or a MLT system for short.

The purpose of making dimensional analysis is to reduce variables and group them in dimensionless form; dimensional analysis has several side benefits (Douglas et al. 2000).

- The first is an enormous saving in time and money.
- A second side benefit of dimensional analysis is that it helps our thinking and planning for an experiment or theory.

- A third benefit is that dimensional analysis provides scaling laws which can convert data from a cheap, small model into design information for an expensive, large prototype.

Many empirical formulas have been developed in the past to estimate the pressure fluctuation beneath hydraulic jump. The dimensionless parameters are used in the prediction formula very widely and there is, as yet, no general agreement regarding the basic non-dimensional parameters affecting the pressure fluctuation beneath hydraulic jump. It is important to recognize that the selection or omission of a certain dimensionless group is critical because a wrong choice often gives an apparent effect in the correlation of data, and results in relationships that are misleading. Considering the case of equilibrium the pressure fluctuation beneath hydraulic jump condition, the set of characteristic parameters appropriate for this fluctuating phenomenon may be listed as follows:

$$C_p^{'} = f(y_t, y_1, u_1, x, g, \rho) \tag{3.4}$$

where ($C'p$) is the pressure fluctuation, (u_1) is the upstream velocity of water issuing from the gate, (y_t) is the tail water depth, (x) is the distance from the gate to the pressure fluctuation measuring point, (y_1) is the gate opening, (g) is the gravitational acceleration and (ρ) is the density of water.

Dimensions of each variable are:

$C_p^{'}$	y_1	y_t	x	U_1	g	ρ
$ML^{-1}T^{-2}$	L	L	L	LT^{-1}	LT^{-2}	ML^{-3}

Using the Buckingham pi theorem;

$$\Pi 4 = f\ (\Pi_1, \Pi_2, \Pi 3) \tag{3.5}$$

The pi groups are formed as follows:

$$\Pi 1 = y_1^{a}, \rho^{b}, U_1^{c}, y_t \tag{3.6}$$

$$\Pi 2 = y_1^{a}, \rho^{b}, U_1^{c}, x \tag{3.7}$$

$$\Pi 3 = y_1^{a}, \rho^{b}, U_1^{c}, g \tag{3.8}$$

$$\Pi 4 = y_1^{a}, \rho^{b}, U_1^{c}, \sqrt{\overline{p'^2}} \tag{3.9}$$

For Π_1

$M^0L^0T^0 = (L)^{a}\ (ML^{-3})^{b}\ (LT^{-1})^{c}\ (L)$

$M \rightarrow 0 = b$

$L \rightarrow 0 = a - 3b + c + 1$

$T \rightarrow 0 = -c$

$\underline{a = -1}$ $\underline{b = 0}$ $\underline{c = 0}$

$\Pi_1 = y_1^{-1}, y_t \rightarrow \Pi_1 = yt / y_1$

For Π_2

$M^0L^0T^0 = (L)^{a}\ (ML^{-3})^{b}\ (LT^{-1})^{c}\ (L)$

$M \rightarrow 0 = b$

$L \rightarrow 0 = a - 3b + c + 1$

$T \rightarrow 0 = -c$

<u>a = -1</u> <u>b = 0</u> <u>c = 0</u>

$\Pi_2 = y_1^{-1}, x \rightarrow \Pi_2 = x/y_1$

For Π_3

$M^0L^0T^0 = (L)^a (ML^{-3})^b (LT^{-1})^c (LT^{-2})$

$M \rightarrow 0 = b$

$L \rightarrow 0 = a - 3b + c + 1$

$T \rightarrow 0 = -c - 2$

<u>a = 1</u> <u>b = 0</u> <u>c = -2</u>

$\Pi_3 = y_1, U_1^{-2}, g \rightarrow \Pi_3 = y_1 * g/U_1^2 = 1/Fr^2$

For Π_4

$M^0L^0T^0 = (L)^a (ML^{-3})^b (LT^{-1})^c (ML^{-1}T^{-2})$

$M \rightarrow 0 = b + 1$

$L \rightarrow 0 = a - 3b + c - 1$

$T \rightarrow 0 = -c - 2$

<u>a = 0</u> <u>b = -1</u> <u>c = -2</u>

$\Pi_4 = p, U_1^{-2}, \rho \rightarrow \Pi_4 = p/U_1^2 * \rho$

$\Pi 4 = f(\Pi_1, \Pi_2, \Pi 3)$

Finally, non dimensional equations in functional forms can be obtained as below:

$$C_p^{'} = \frac{\sqrt{\overline{p'^2}}}{1/2\rho_w u_1^2} = f\left(\frac{y_t}{y_1}, \frac{x}{y_1}, \frac{1}{F_1^2}\right) \tag{3.10}$$

CHAPTER 4

DATA COLLECTION AND DATA SET ANALYSIS

In this study, an intensive literature review on experimental studies on pressure fluctuation beneath hydraulic jump has been performed. Unfortunately, most of the studies don't represent their experimental findings in detail, especially the details that conform to our study. We could find three experimental studies:

1. Rinaldo, A. and Fiorotto, V. (1993) "Turbulent pressure fluctuations under hydraulic jumps."
2. Lopardo, R.A., De Lio, J.C., and Lopardo, M.C. (1999). "Physical modeling and design estimation of instantaneous pressures in stilling basins" *Proc. of the 28th IAHR Congress*, Graz.
3. Pirooz B. and Kavianpour M. R. (2005). "Experimental investigation of pressure fluctuations beneath hydraulic jump."

The experimental data used this study are given in Table 4.1 and Table 4.2. Table 4.1 shows the dimensional form of parameters most affecting pressure fluctuation, and Table 4.2 shows the non-dimensional form of these parameters, derived from dimensional analysis (Buckingham Pi Theorem) explained in Chapter 4.

Tables 4.3 and 4.4 show the correlation between the parameters given in Tables 4.1 and 4.2. The correlation was found throughout linear regression, taking mean pressure fluctuation ($\sqrt{\overline{p'^2}}$) and non-dimensional fluctuation parameter as dependent variables and the other variables as independent variables. From Tables 4.3 and 4.4 it is obviously seen that the correlation between both dimensional and non-dimensional parameters are quite poor. This means there is too weak linear correlation between the parameters and non-linear analysis techniques should be applied in order to achieve better results.

Table 4.1: Summary of experimental data

Researchers	u_1 (m/s)	y_t (m)	y_1(m)	x (m)	$\sqrt{\overline{p'^2}}$ (Pa)
	3,55	0,24	0,025	0,175	0,0417
	3,55	0,24	0,025	0,22	0,045
	3,55	0,24	0,025	0,27	0,054
	3,55	0,24	0,025	0,32	0,0615
	3,55	0,24	0,025	0,34	0,059
	3,55	0,24	0,025	0,36	0,0625
	3,55	0,24	0,025	0,37	0,053
	3,55	0,24	0,025	0,39	0,0626
	3,55	0,24	0,025	0,42	0,0621
	3,55	0,24	0,025	0,44	0,0582
	3,55	0,24	0,025	0,46	0,0558
	3,55	0,24	0,025	0,48	0,0542
	3,55	0,24	0,025	0,51	0,0508
	3,55	0,24	0,025	0,53	0,0452
	3,55	0,24	0,025	0,55	0,0434
	1,88	0,22	0,027	0,32	0,078
	1,88	0,22	0,027	0,37	0,0815
	1,88	0,22	0,027	0,39	0,083
	1,88	0,22	0,027	0,43	0,082
	1,88	0,22	0,027	0,46	0,081
Virgilio Fiorotto	1,88	0,22	0,027	0,49	0,08
Andrea Rinaldo (1993)	1,88	0,22	0,027	0,52	0,076
	1,88	0,22	0,027	0,56	0,0725
	1,88	0,22	0,027	0,59	0,078
	1,88	0,22	0,027	0,62	0,065
	1,88	0,22	0,027	0,65	0,073
	1,88	0,22	0,027	0,68	0,074
	1,88	0,22	0,027	0,71	0,079
	1,88	0,22	0,027	0,74	0,073
	1,88	0,22	0,027	0,78	0,0635
	1,88	0,22	0,027	0,81	0,064
	1,88	0,22	0,027	0,84	0,058
	1,88	0,22	0,027	0,86	0,06
	3,61	0,25	0,034	0,23	0,068
	3,61	0,25	0,034	0,26	0,067
	3,61	0,25	0,034	0,28	0,073
	3,61	0,25	0,034	0,298	0,077
	3,61	0,25	0,034	0,32	0,067
	3,61	0,25	0,034	0,34	0,072
	3,61	0,25	0,034	0,36	0,071
	3,61	0,25	0,034	0,38	0,076

	3,61	0,25	0,034	0,4	0,082
	3,61	0,25	0,034	0,43	0,077
	3,61	0,25	0,034	0,45	0,078
	3,61	0,25	0,034	0,48	0,0765
	3,61	0,25	0,034	0,51	0,0775
	3,61	0,25	0,034	0,52	0,076
	3,61	0,25	0,034	0,54	0,077
	3,61	0,25	0,034	0,56	0,0765
	3,61	0,25	0,034	0,59	0,0755
	3,61	0,25	0,034	0,61	0,074
	3,71	0,19	0,03	0,24	0,078
	3,71	0,19	0,03	0,26	0,0795
	3,71	0,19	0,03	0,28	0,076
	3,71	0,19	0,03	0,29	0,081
	3,71	0,19	0,03	0,32	0,079
	3,71	0,19	0,03	0,33	0,0815
	3,71	0,19	0,03	0,35	0,082
	3,71	0,19	0,03	0,37	0,0815
	3,71	0,19	0,03	0,38	0,08
	3,71	0,19	0,03	0,41	0,083
	3,71	0,19	0,03	0,43	0,08
	3,71	0,19	0,03	0,45	0,0805
	3,71	0,19	0,03	0,47	0,0785
	3,71	0,19	0,03	0,48	0,071
	3,71	0,19	0,03	0,51	0,0735
	3,71	0,19	0,03	0,52	0,073
	3,71	0,19	0,03	0,53	0,072
	1,38	0,45	0,035	0,525	0,036
Virgilio Fiorotto	1,38	0,45	0,035	0,58	0,039
Andrea Rinaldo (1993)	1,38	0,45	0,035	0,64	0,041
	1,38	0,45	0,035	0,69	0,043
	1,38	0,45	0,035	0,75	0,0425
	1,38	0,45	0,035	0,81	0,047
	1,38	0,45	0,035	0,85	0,046
	1,38	0,45	0,035	0,91	0,0442
	1,38	0,45	0,035	0,97	0,0455
	1,38	0,45	0,035	1,01	0,045
	1,38	0,45	0,035	1,07	0,046
	1,38	0,45	0,035	1,13	0,048
	1,38	0,45	0,035	1,15	0,0415
	1,38	0,45	0,035	1,24	0,04
	1,38	0,45	0,035	1,29	0,0418
	1,38	0,45	0,035	1,35	0,0398
	1,38	0,45	0,035	1,41	0,039
	1,38	0,45	0,035	1,47	0,0395

	2,72	0,127	0,012	0	0,026
	2,72	0,127	0,012	0,035	0,042
	2,72	0,127	0,012	0,07	0,028
	2,72	0,127	0,012	0,094	0,05
B. Pirooz and	2,72	0,127	0,012	0,118	0,07
M.R. Kavianpour (2005)	2,72	0,127	0,012	0,153	0,094
	2,72	0,127	0,012	0,288	0,10
	2,72	0,127	0,012	0,247	0,082
	2,72	0,127	0,012	0,283	0,08
	2,72	0,127	0,012	0,486	0,086
	2,72	0,127	0,012	0,542	0,084
	2,72	0,127	0,012	0,365	0,066
	2,72	0,127	0,012	0,389	0,059
	2,72	0,127	0,012	0,413	0,046
	2,72	0,127	0,012	0,448	0,045
	2,72	0,127	0,012	0,495	0,05
	2,72	0,127	0,012	0,519	0,045
	2,72	0,127	0,012	0,542	0,048
	2,72	0,127	0,012	0,578	0,036
	2,72	0,127	0,012	0,601	0,035
	2,72	0,127	0,012	0,613	0,03
	2,72	0,127	1,180	0,637	0,03
	25,60	25,30	4,200	0,000	0,027
	25,60	25,30	4,200	4,28	0,03
	25,60	25,30	4,200	5,35	0,035
	25,60	25,30	4,200	8,54	0,033
	25,60	25,30	4,200	10,70	0,037
	25,60	25,30	4,200	13,90	0,045
	25,60	25,30	4,200	17,12	0,045
	25,60	25,30	4,200	19,26	0,042
	25,60	25,30	4,200	22,47	0,047
	25,60	25,30	4,200	25,68	0,055
	25,60	25,30	4,200	27,82	0,055
	25,60	25,30	4,200	31,03	0,05
	25,60	25,30	4,200	33,17	0,045
	25,60	25,30	4,200	38,52	0,047
	25,60	25,30	4,200	43,87	0,043
Raul A.Lopardo,	25,60	25,30	4,200	50,29	0,037
Julio C. De Lio	25,60	25,30	4,200	55,64	0,035
Maria C. Lopardo (1999)	25,60	25,30	4,200	62,06	0,03
	25,60	25,30	4,200	66,34	0,27
	25,60	25,30	4,200	72,76	0,29
	25,60	25,30	4,200	79,18	0,025
	25,60	25,30	4,200	83,46	0,022
	25,60	25,30	4,200	86,67	0,024

	25,6	25,30	4,200	94,16	0,02
	25,93	25,44	4,200	5,35	0,045
	25,93	25,44	4,200	10,7	0,05
	25,93	25,44	4,200	17,12	0,06
	25,93	25,44	4,200	21,4	0,067
	25,93	25,44	4,200	24,61	0,067
	25,93	25,44	4,200	31,03	0,063
	25,93	25,44	4,200	34,24	0,06
	25,93	25,44	4,200	38,52	0,055
	25,93	25,44	4,200	49,22	0,045
	25,93	25,44	4,200	57,78	0,032
	25,93	25,44	4,200	78,11	0,02
	25,93	25,44	4,200	93,09	0,017
	26,75	17,01	2,600	0	0,025
	26,75	17,01	2,600	2,775	0,027
	26,75	17,01	2,600	4,625	0,037
	26,75	17,01	2,600	7,40	0,035
	26,75	17,01	2,600	10,175	0,04
	26,75	17,01	2,600	12,95	0,042
	26,75	17,01	2,600	14,80	0,045
	26,75	17,01	2,600	17,575	0,042
	26,75	17,01	2,600	20,35	0,047
	26,75	17,01	2,600	22,20	0,046
	26,75	17,01	2,600	24,975	0,046
	26,75	17,01	2,600	27,75	0,04
	26,75	17,01	2,600	29,60	0,037
	26,75	17,01	2,600	35,15	0,035
	26,75	17,01	2,600	39,775	0,032
	26,75	17,01	2,600	45,325	0,03
	26,75	17,01	2,600	49,95	0,027
	26,75	17,01	2,600	54,575	0,025
	26,75	17,01	2,600	60,125	0,022
	26,75	17,01	2,600	64,75	0,022
	26,75	17,01	2,600	70,30	0,021
	26,75	17,01	2,600	74,925	0,02
Raul A.Lopardo	26,75	17,01	2,600	78,625	0,016
Julio C. De Lio	26,75	17,01	2,600	84,175	0,015
Maria C. Lopardo (1999)	26,75	17,01	2,600	88,80	0,01
	28,78	18,30	2,600	3,70	0,033
	28,78	18,30	2,600	6,475	0,045
	28,78	18,30	2,600	10,175	0,053
	28,78	18,30	2,600	12,95	0,058
	28,78	18,30	2,600	16,65	0,065
	28,78	18,30	2,600	20,35	0,068
	28,78	18,30	2,600	23,125	0,069

	28,78	18,30	2,600	26,825	0,069
	28,78	18,30	2,600	30,525	0,06
	28,78	18,30	2,600	33,30	0,055
	28,78	18,30	2,600	37	0,05
	28,78	18,30	2,600	41,625	0,048
	28,78	18,30	2,600	43,475	0,042
	28,78	18,30	2,600	55,50	0,03
	28,78	18,30	2,600	57,35	0,027
	28,78	18,30	2,600	61,975	0,025
	28,78	18,30	2,600	63,825	0,024
	28,78	18,30	2,600	67,525	0,02
	28,78	18,30	2,600	68,45	0,02
	28,78	18,30	2,600	72,15	0,017
	28,78	18,30	2,600	74,925	0,016
	28,78	18,30	2,600	80,475	0,02
	28,78	18,30	2,600	86,95	0,015

Table 4.2. Non-dimensional form of data

Researchers	$1/F_1^2$	y_t / y_1	x/ y_1	$C_p^{'}$
	0,019	9,69	7	0,0417
	0,019	9,69	8,75	0,045
	0,019	9,69	10,7	0,054
	0,019	9,69	12,6	0,0615
	0,019	9,69	13,45	0,059
	0,019	9,69	14,1	0,0625
	0,019	9,69	14,9	0,053
	0,019	9,69	15,8	0,0626
	0,019	9,69	16,6	0,0621
	0,019	9,69	17,6	0,0582
	0,019	9,69	18,5	0,0558
	0,019	9,69	19,35	0,0542
	0,019	9,69	20,2	0,0508
	0,019	9,69	21,15	0,0452
	0,019	9,69	22	0,0434
	0,025	8,42	12	0,078
	0,025	8,42	13,7	0,0815
	0,025	8,42	14,7	0,083
	0,025	8,42	16,1	0,082
	0,025	8,42	17,2	0,081
Virgilio Fiorotto	0,025	8,42	18,3	0,08
Andrea Rinaldo (1993)	0,025	8,42	19,5	0,076
	0,025	8,42	20,6	0,0725
	0,025	8,42	21,8	0,078
	0,025	8,42	23	0,065
	0,025	8,42	24,2	0,073
	0,025	8,42	25,3	0,074
	0,025	8,42	26,5	0,079
	0,025	8,42	27,6	0,073
	0,025	8,42	28,8	0,0635
	0,025	8,42	29,9	0,064
	0,025	8,42	31	0,058
	0,025	8,42	32	0,06
	0,03	7,58	7	0,068
	0,03	7,58	7,65	0,067
	0,03	7,58	8,25	0,073
	0,03	7,58	8,8	0,077
	0,03	7,58	9,5	0,067
	0,03	7,58	10,2	0,072
	0,03	7,58	10,7	0,071
	0,03	7,58	11,4	0,076

	0,030	7,58	12	0,082
	0,030	7,58	12,75	0,077
	0,030	7,58	13,45	0,078
	0,030	7,58	14,15	0,0765
	0,030	7,58	14,87	0,0775
	0,030	7,58	15,38	0,076
	0,030	7,58	16	0,077
	0,030	7,58	16,6	0,0765
	0,030	7,58	17,35	0,0755
	0,030	7,58	18	0,074
	0,040	6,59	8	0,078
	0,040	6,59	8,75	0,0795
	0,040	6,59	9,35	0,076
	0,040	6,59	9,9	0,081
	0,040	6,59	10,5	0,079
	0,040	6,59	11,15	0,0815
	0,040	6,59	11,7	0,082
	0,040	6,59	12,3	0,0815
	0,040	6,59	12,8	0,08
	0,040	6,59	13,75	0,083
	0,040	6,59	14,4	0,08
	0,040	6,59	15	0,0805
	0,040	6,59	15,6	0,0785
	0,040	6,59	16,1	0,071
	0,040	6,59	16,7	0,0735
	0,040	6,59	17,3	0,073
	0,040	6,59	17,8	0,072
	0,011	12,94	15	0,036
	0,011	12,94	16,6	0,039
Virgilio Fiorotto	0,011	12,94	18,2	0,041
Andrea Rinaldo (1993)	0,011	12,94	19,9	0,043
	0,011	12,94	21,5	0,0425
	0,011	12,94	23	0,047
	0,011	12,94	24,4	0,046
	0,011	12,94	26	0,0442
	0,011	12,94	27,6	0,0455
	0,011	12,94	29	0,045
	0,011	12,94	30,6	0,046
	0,011	12,94	32,2	0,048
	0,011	12,94	33,8	0,0415
	0,011	12,94	35,4	0,04
	0,011	12,94	37	0,0418
	0,011	12,94	38,6	0,0398
	0,011	12,94	40,4	0,039

	0,047	6,02	22,41	0,02
	0,046	6,06	1,273	0,045
	0,046	6,06	2,54	0,05
	0,046	6,06	4,078	0,06
	0,046	6,06	5,09	0,067
	0,046	6,06	5,86	0,067
	0,046	6,06	7,39	0,063
	0,046	6,06	8,15	0,06
	0,046	6,06	9,17	0,055
	0,046	6,06	11,72	0,045
	0,046	6,06	13,76	0,032
	0,046	6,06	18,6	0,02
	0,046	6,06	22,16	0,017
	0,035	6,54	0	0,025
	0,035	6,54	1,067	0,027
	0,035	6,54	1,778	0,037
	0,035	6,54	2,846	0,035
	0,035	6,54	3,91	0,04
	0,035	6,54	4,98	0,042
	0,035	6,54	5,7	0,045
	0,035	6,54	6,76	0,042
	0,035	6,54	7,83	0,047
	0,035	6,54	8,54	0,046
	0,035	6,54	9,6	0,046
	0,035	6,54	10,76	0,04
	0,035	6,54	11,38	0,037
	0,035	6,54	13,52	0,035
	0,035	6,54	15,29	0,032
	0,035	6,54	17,43	0,03
	0,035	6,54	19,21	0,027
	0,035	6,54	21	0,025
	0,035	6,54	23,125	0,022
	0,035	6,54	24,9	0,022
	0,035	6,54	27,93	0,021
	0,030	7,04	41,74	0,06
	0,035	6,54	28,81	0,02
Raul A.Lopardo,	0,035	6,54	30,24	0,016
Julio C. De Lio and	0,035	6,54	32,375	0,015
Maria C. Lopardo (1999)	0,035	6,54	34,15	0,01
	0,030	7,04	1,42	0,033
	0,030	7,04	2,5	0,045
	0,030	7,04	3,91	0,053
	0,030	7,04	4,98	0,058
	0,030	7,04	6,4	0,065
	0,030	7,04	7,826	0,068
	0,030	7,04	12,80	0,055

	0,030	7,04	14,23	0,05
	0,030	7,04	24,55	0,024
	0,030	7,04	25,97	0,02
	0,030	7,04	16,00	0,048
	0,030	7,04	16,72	0,042
	0,030	7,04	21,34	0,03
	0,030	7,04	22,05	0,027
	0,030	7,04	23,83	0,025
	0,030	7,04	8,89	0,069
	0,030	7,04	10,31	0,069
	0,030	7,04	26,32	0,02
	0,030	7,04	27,75	0,017
	0,030	7,04	28,82	0,016
	0,030	7,04	30,95	0,02
	0,030	7,04	33,44	0,015
	0,015	10,82	0	0,026
	0,015	10,82	3	0,042
	0,015	10,82	6	0,028
B.Pirooz	0,015	10,82	8	0,05
M.R. Kavianpour (2005)	0,015	10,82	10	0,07
	0,015	10,82	13	0,094
	0,015	10,82	16	0,1
	0,015	10,82	21	0,082
	0,015	10,82	24	0,08
	0,015	10,82	27	0,086
	0,015	10,82	29	0,084
	0,015	10,82	31	0,066
	0,015	10,82	33	0,059
	0,015	10,82	35	0,046
B.Pirooz	0,015	10,82	38	0,045
M.R. Kavianpour (2005)	0,015	10,82	42	0,05
	0,015	10,82	44	0,045
	0,015	10,82	46	0,048
	0,015	10,82	49	0,036
	0,015	10,82	51	0,035
	0,015	10,82	52	0,03
	0,015	10,82	54	0,03
	0,047	6,02	0	0,027
	0,047	6,02	1,02	0,03
	0,047	6,02	1,273	0,035
	0,047	6,02	2,03	0,033
	0,047	6,02	2,55	0,037
	0,047	6,02	4,076	0,045
	0,047	6,02	3,31	0,045
	0,047	6,02	4,58	0,042
	0,047	6,02	5,35	0,047

	0,047	6,02	6,62	0,055
	0,047	6,02	7,39	0,05
	0,047	6,02	7,89	0,045
	0,047	6,02	9,17	0,047
	0,047	6,02	10,44	0,043
	0,047	6,02	11,97	0,037
	0,047	6,02	13,24	0,035
	0,047	6,02	14,77	0,03
Raul A.Lopardo	0,047	6,02	15,79	0,27
Julio C. De Lio	0,047	6,02	17,32	0,29
Maria C. Lopardo (1999)	0,047	6,02	18,85	0,025

Table 4.3. Correlation between mean pressure fluctuation and input parameters.

	u_1	y_t	y_1	x	$\sqrt{\overline{p'^2}}$
u_1	1				
y_t	-0,270	1			
y_1	0,318382	0,599935	1		
x	-0,24402	0,542724	0,140695	1	
$\sqrt{\overline{p'^2}}$	0,652848	-0,1135	0,306567	-0,19772	1

Table 4.4 Correlation between dimensionless pressure fluctuation parameter and input parameters.

	$(1/F_1)$	(y_t/y_1)	(x/y_1)	(C_p')
$(1/F_1)$	1			
(y_t/y_1)	-0,932611471	1		
(x/y_1)	-0,543398835	0,537937464	1	
(C_p')	0,048691325	-0,135385667	-0,033474758	1

CHAPTER 5

ARTIFICIAL NEURAL NETWORKS

5.1 General

Artificial Neural Networks are computer models that mimic the biological nervous system. A neural network can be defined a massively parallel distributed processor that has a natural tendency for storing experiential knowledge and making it available for use (Haykin 2000). The main component of this model is the structure of its information processing unit. The biological neuron model (see Figure 5.1) is also the basis of the artificial neuron model. A biological neuron is made up of four main parts: dendrites, synapses, axon and the cell body. The dendrites receive signals from other neurons. The axon of a single neuron serves to form synaptic connections with other neurons. The cell body of a neuron sums the incoming signals from dendrites. If input signals are sufficient to stimulate the neuron to its threshold level, the neuron sends an impulse to its axon. On the other hand if the inputs do not reach the required level, no impulse will occur (Haykin 2000).

The first application in Civil Engineering only goes back to the late of 1980s, Levitt et al. (1988) and Flood (1989). Some of the first applications of artificial neural network in water engineering were carried out by Karunanithi and co-workers in 1994 in

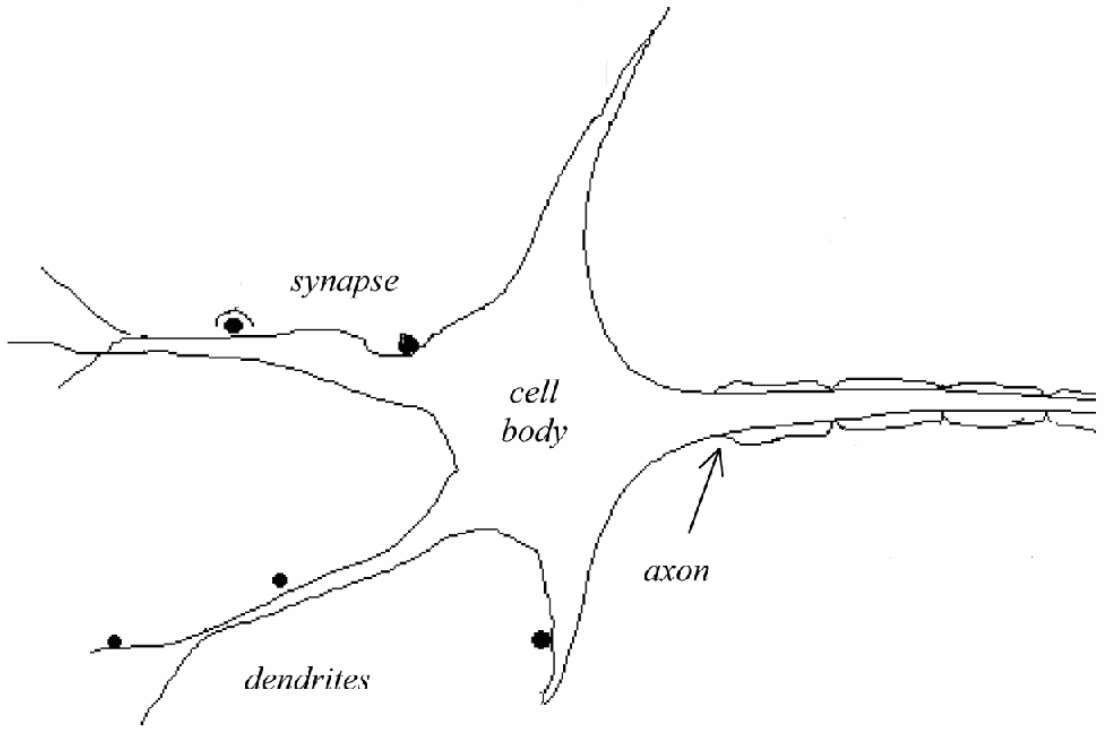

Figure 5.1 A biological neuron model

predicting the river flow and Grubert in 1995 in the stability analysis of stratified flow. Most of the ANN applications in water engineering can be found in ASCE task Committee (2000), Maier and Dandy (2000), Negm (2001), Negm and Shouman (2002), and Dolling and Varas (2002). Therefore, some recent studies were additionally reviewed in this study. ANNs were applied by Liu and James (2000) in estimation of discharge capacity in meandering compound channels, by Baxter et al. (2001) in evaluating the drinking water quality, by Nagy et al. (2002) in prediction of sediment load concentration in rivers, by Sarghini et al. (2003) in modelling of turbulent flows in co-operation with large eddy simulation, and by Azmatullah et al. (2006) in prediction of scour below spillways.

5.2 Multilayer Neural Networks

Multilayer neural networks (Figure 5.3) are undoubtedly the most popular networks used in applications. While it is possible to consider many activation functions, in practice it has been found that the logistic (also called the sigmoid) function:

$$y(x) = \frac{1}{1+e^{-x}} \tag{5.3}$$

as the activation function (or variants such as the tanh function) works best. In this study, tangent hyperbolic function was used. In fact the revival of interest in neural nets was sparked by successes in training neural networks using this function in place of the historically (biologically inspired) step function (the "perceptron") (Rosenblatt, 1957). Notice that using a linear function does not achieve anything in multilayer networks that is beyond what can be done with single layer networks with linear activation functions. The practical value of the logistic function arises from the fact that it is almost linear in the range where y is between 0.1 and 0.9 but has a squashing effect on very small or very large values of x (Bishop, 1995).

The basic element of a NN is an artificial neuron as shown in Figure 5.2, which consists of three main components; weights, bias, and an activation function. Each neuron receives inputs x_i (i = 1, 2, …, n) attached with a weight w_{ij} ($j \geq 1$) which shows the connection strength for a particular input for each connection. Every input is then multiplied by the corresponding weight of the neuron connection and summed as

$$W_i = \sum_{j=1}^{n} w_{ij} x_j \tag{5.4}$$

A bias b_i, a type of correction weight with a constant non-zero value, is added to the summation in Equation (5.5) as

$$U_i = W_i + b_i \tag{5.5}$$

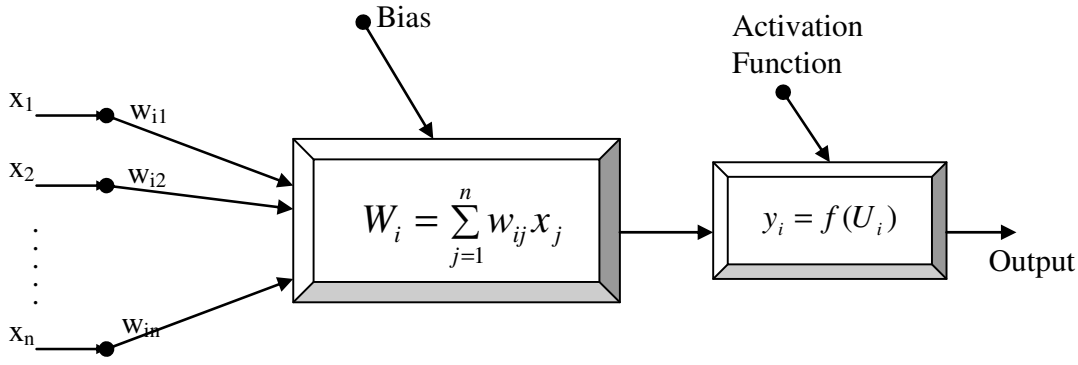

Figure 5.2 An artificial neuron model.

In other word, W_i in Equation (5.5) is the weighted sum of the i^{th} neuron for the input received from the preceding layer with n neurons, w_{ij} is the weight between the i^{th} neuron in the hidden layer and the j^{th} neuron in the preceding (input) layer, and x_j is the output of the j^{th} neuron in the input layer. After being corrected by a bias as in Equation (2), the summation is transferred using a scalar-to-scalar function called an "activation or transfer function", $f(U_i)$, to yield a value called the unit's "activation", given as

$$y_i = f(U_i) \tag{5.6}$$

Activation functions serve to introduce nonlinearity into NNs which makes it more powerful than linear transformation.

In theory it is sufficient to consider networks with two layers of neurons– one hidden and one output layer–and this is certainly the case for most applications. There are, however, a number of situations where three and sometimes four and five layers have been more effective. In this study, we tried several numbers of layers and observed

that increasing number of layers did not improve the predictions of the network in considerable amount. For prediction the output node is often given a linear activation function to provide forecasts that are not limited to the zero to one range. An alternative is to scale the output to the linear part (0.1 to 0.9) of the logistic function.

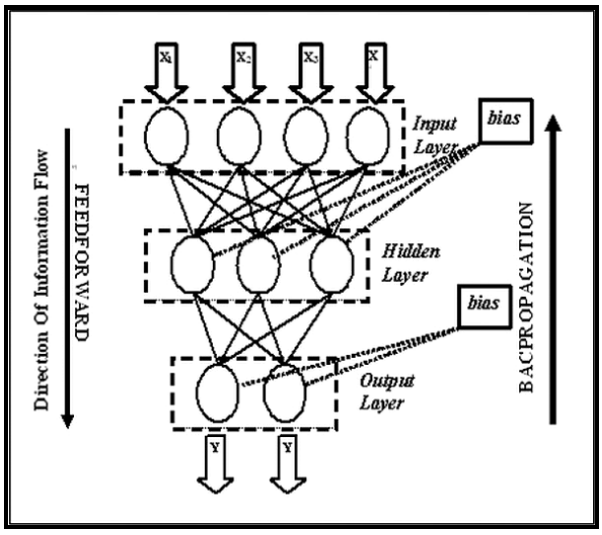

Figure 5.3. A multilayer feed forward neural network with back propagation (Çevik, 2006)

Unfortunately there is no clear theory to guide us on choosing the number of nodes in each hidden layer or indeed the number of layers. The common practice is to use trial and error, although there are schemes for combining optimization methods such as genetic algorithms with network training for these parameters. Since trial and error is a necessary part of neural net applications it is important to have an understanding of the standard method used to train a multilayered network: backpropagation. It is no exaggeration to say that the speed of the backprop algorithm made neural nets a practical tool in the manner that the simplex method made linear optimization a practical tool.

The revival of strong interest in neural nets in the mid 80s was in large measure due to the efficiency of the backprop algorithm (Bishop, 1995).

5.3 Back Propagation Algorithm

Back propagation algorithm is one of the most widely used supervised training methods for training multilayer neural networks due to its simplicity and applicability. It is based on the generalized delta rule and was popularized by Rumelhart and co-workers (Rumelhart et al. 1986). As it is a supervised learning algorithm, there is a pair of inputs and corresponding output. The algorithm is simply based on a weight correction procedure. It consists of two passes: a forward pass and a backward pass. In the forward pass, first, the weights of the network are randomly initialized and an output set is obtained for a given input set where weights are kept as fixed. The error between the output of the network and the target value is propagated backward during the backward pass and used to update the weights of the previous layers as shown in Figure 5.3 (Haykin 2000, Hebb 1949, Minsky and Pappert 1949, Rumelhart et al. 1986, Zupan and Gasteiger 1993, Çevik 2006).

CHAPTER 6

NEURAL NETWORKS APPLICATION

6.1 Building neural networks architecture

The main focus of this study is to predict the mean pressure fluctuations beneath hydraulic jump occurring horizontal channels by means of ANNs based on experimental results. The experimental results were derived from other studies from the literature. Two neural network models are proposed, namely the first model predicts mean pressure fluctuation, $\sqrt{\overline{p'^2}}$, as a function of basic geometrical and incoming flow variables affecting the pressure fluctuation. The second model predicts the non-dimensional pressure fluctuation parameter, $C_p^{'}$, as a function of non-dimensional parameters derived from dimensional analysis using the same physical variables used in the first model. The variables used in the experimental study are given in Tables 4.1 and 4.2. These experimental tests were used as training and test sets for both NN training. Among these 192 tests 38 tests (20% of total) were used as test set and the remaining as training set for NN training. The ranges of variables are presented in Table 6.1.

Table 6.1. Minimum and maximum values for canal section variables.

Variable	Minimum value	Maximum value
Gate opening (y_1)	1.18 *mm*	4.2 *mm*
Upstream velocity of water issuing from the gate (u_1)	1.38 m/s	28.78 m/s
Tail water depth (y_t)	1.18 *mm*	45.43 *mm*
The distance from the aget to pressure fluctuation measuring point (x)	0 *mm*	147.42 *mm*
Pressure fluctuation ($\overline{\sqrt{p'^2}}$)	34.23 Pa	95027.20 Pa

6.2 Optimal neural networks architecture

One of the most important tasks in NN studies is to determine the optimal network architecture which is related to the number of neurons in the hidden layer. Generally, the trial and error approach is used. In this study, the best architectures of the networks were obtained by trying different number of neurons. The trial started from two, and the performance of each network was checked by employing Mean Absolute Percentage Error (MAPE) defined as

$$\text{MAPE} = \left(\left| \frac{X - Y}{Y} \right| x100 \right) / n \tag{6.1}$$

where n is the number of exemplars in the training set, X is the observed pressure fluctuation parameter values and Y is the predicted pressure fluctuation parameter

values. MAPE is used to measure the exchange between training performance and network size. The goal is to minimize MAPE to obtain a network with the best generalization.

The relationship between the number of neurons ranging from 2 to 20 and the corresponding MAPE values obtained is presented in Figures 6.1 and 6.2. It is seen in Figure 6.1a that MAPE values decrease with increasing number of neurons in the training stage. Therefore, the architecture of the network improves in the learning process with increasing number of neurons. In the testing process, however, MAPE values reduce with increasing number of neurons until the number of neurons reaches sixteen and then the MAPE values start to increase, which implies that the network becomes more generalized with increasing number of neurons until an optimum value is obtained. Beyond this optimum point the network turns out to be specialized only on the training set and it deviates from producing reasonable results in the testing stage. This procedure is a common experience in NN studies. The same findings are observed in Figure 6.2(a), namely, MAPE values reduce with increasing number of neurons until the number of neurons reaches seventeen and then the MAPE values start to increase.

The coefficient of determination, R^2, is also shown in Figures 6.1b and 6.2b. The correlation coefficient seems to be slightly affected by increasing number of neurons in the training stage (Figure 6.1b) up to sixteen neurons beyond which no change was noticed. However, Figure 6.1b shows that R^2 starts to decrease with increase in the number of neurons after the sixteenth neuron and Figure 6.2b shows that R^2 starts to decrease with number of neurons after the seventeenth neuron. Based on these analyses, the optimal architecture was constructed as 4-16-1 for NN based on dimensional

parameters and 3-17-1 for NN based on non-dimensional parameters, representing the number of inputs, neurons, and outputs, respectively (Figures 6.3 and 6.4).

In the architecture the tangent-sigmoid transfer function is utilized as:

$$y_i = f(U_i) = \frac{2}{1+e^{-2U_i}} - 1 \tag{6.2}$$

Most of the engineering applications of the NNs are based on back-propagation training algorithm (ASCE Task Committee, 2000). In this study, the Levenberg-Marquardt back-propagation algorithm was employed to minimize the *MSE* of the network.

$$MSE = \sum (X - Y)^2 / n \tag{6.3}$$

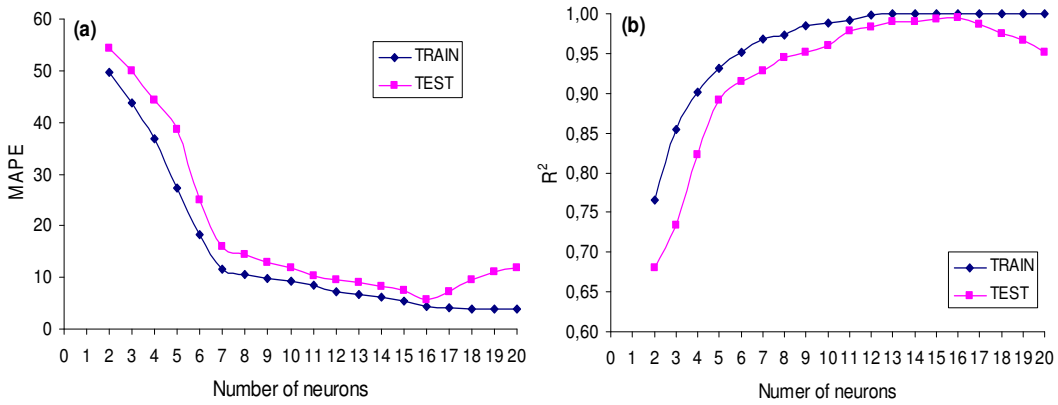

Figure 6.1. The effect of number of neurons on the NN1 performance for training and testing sets

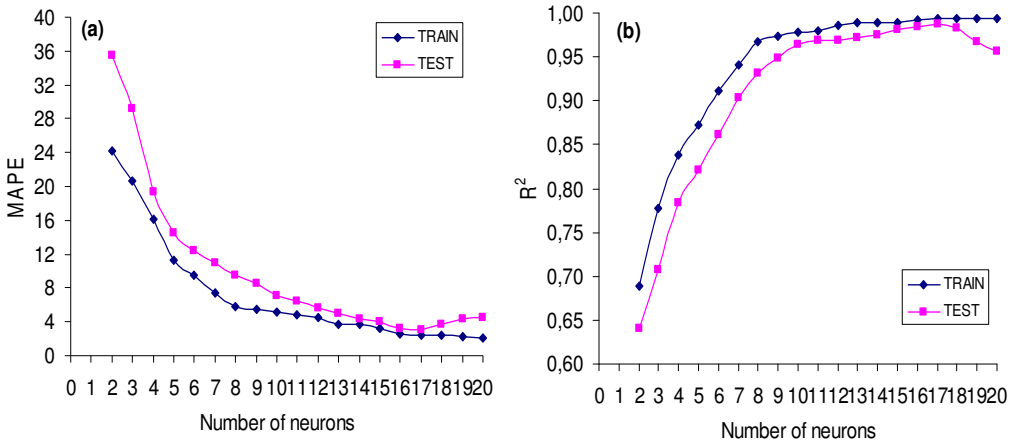

Figure 6.2. The effect of number of neurons on the NN2 performance for training and testing sets

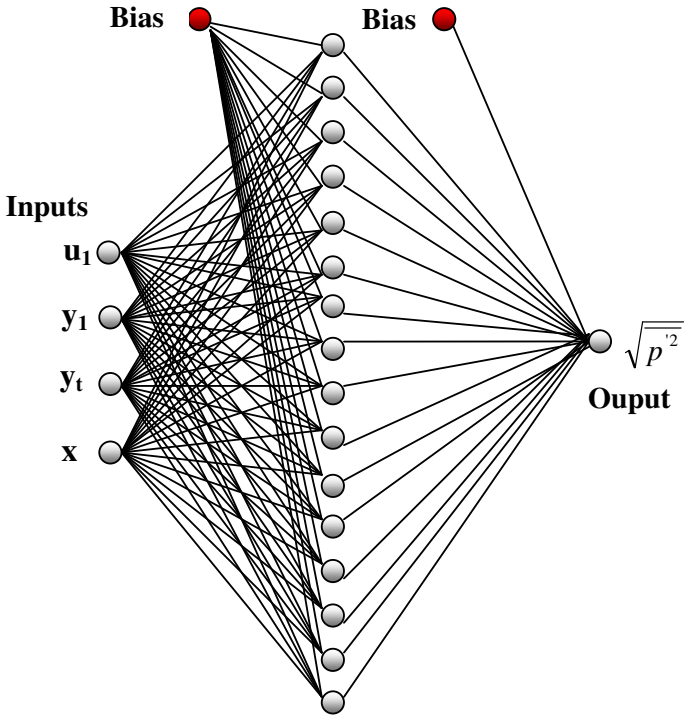

Figure 6.3. Optimum NN Architecture based on dimensional parameters

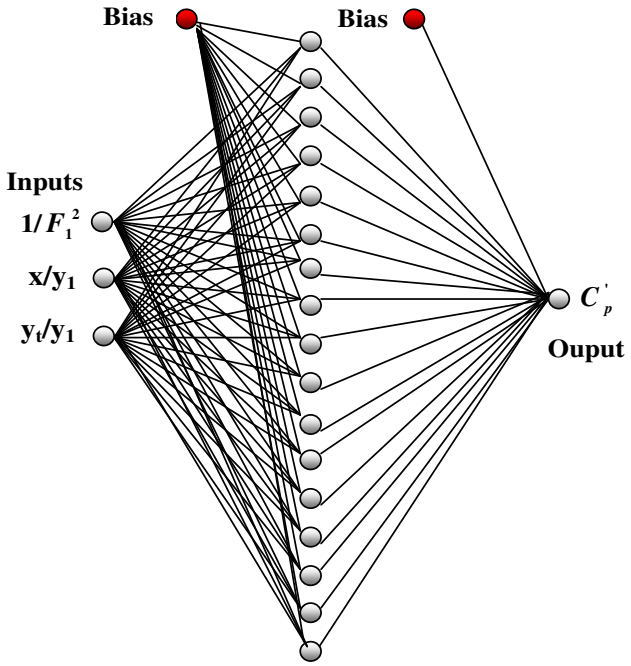

Fig. 6.4. Optimum NN Architecture based on non-dimensional parameters

6.3 Training and testing the proposed neural networks

The data taken from the three studies were used as training and testing sets (192 in total) for the chosen NN architectures. Among these, 38 tests (20% of total) were reserved for the test set and the remaining data were perceived in the training. The overall performances of both sets were evaluated by *MAPE* – the slope *a* and intercept *b* of the best-fit linear line – and the determination coefficient (R^2).

Figure 6.5 compares the NN estimates to the experimental data via scatter plots for training (Figure 6.5a) and testing sets (Figure 6.5b). It is clearly noted in Figure 6.5 that the proposed NN model has impressively well learned the nonlinear relationship between the input and the output variables with *MAPE* = 4.372 (a = 0.9972, b = 2.802) and R^2 = 0.999. Comparing the NN predictions with the experimental data for the test stage demonstrates a high generalization capacity of the proposed model with relatively

low error and high correlation (*MAPE* =5.690, a = 1.0534, b = -287.42 and R^2 = 0.995), which exhibits a successful performance of the NNs model for estimating the pressure fluctuation both in training and testing stages (Figure 6.5b). Figure 6.6 show similar findings for NN estimates to non-dimensional data. Statistical results of both neural networks model in training and testing stages arge given in Table 6.2

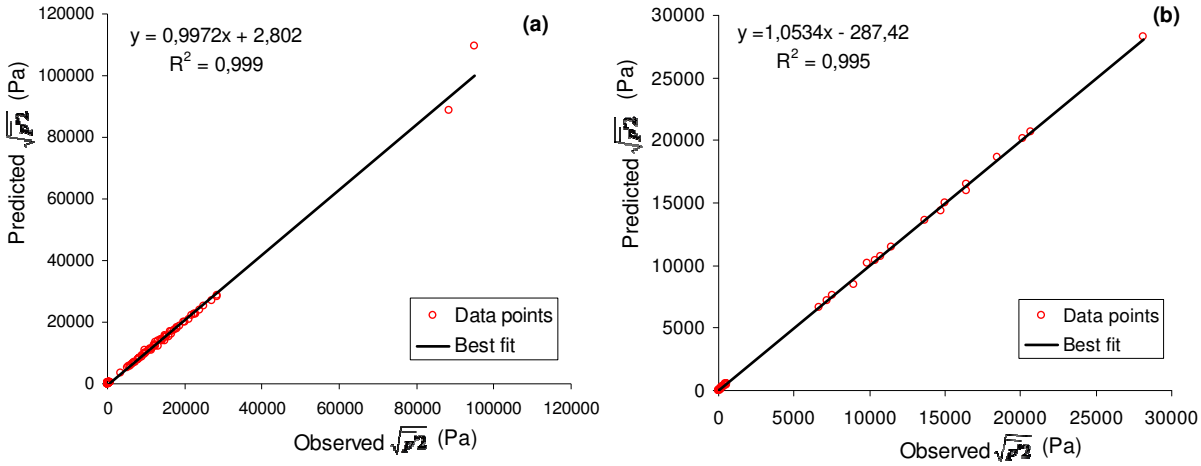

Figure 6.5 Comparison of NN predictions with experimental mean pressure fluctuation

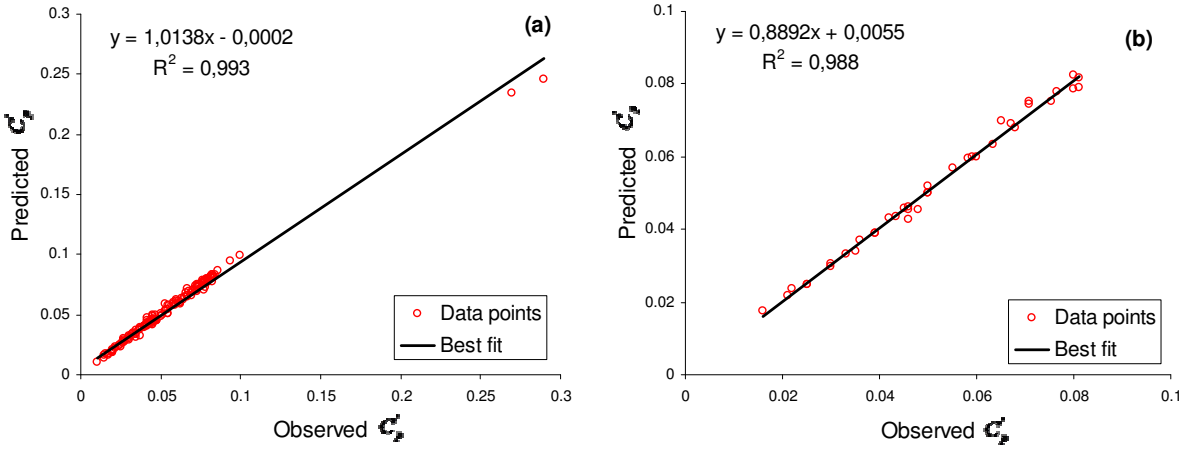

Figure 6.6. Comparison of NN predictions with experimental non-dimensional pressure fluctuation parameter

Table 6.2. Statistical Parameters of Optimum NN models

		RMSE	SSE	MAPE (%)	Correlation Coefficient (R)
Dimensional	Test Set	0.0015	0.0043	7.1276	0.987
	Training set	0.0009	0.0022	4.1291	0.999
Dimensionless	Test Set	0.0019	0.0028	3.0629	0.988
	Training set	0.0012	0,.0031	2.4979	0.993

Note: R (Correlation coefficient)= $\sum xy / \sqrt{\sum x^2 \sum y^2}$, $x = X - X^{'}; y = Y - Y^{'}$; X = observed pressure fluctuation parameter values, $X^{'}$ = mean of *X*, *Y* = predicted pressure fluctuation parameter values, $Y^{'}$ = mean of *Y*; RMSE (Root Mean Square Error)= $\left[\sum (X-Y)^2 / n\right]^{1/2}$, and SSE (Sum Squared Error)= $\sum (X-Y)^2$

6.4 Explicit Neural Networks Formulation (ENNF)

The aim of this study is to derive an explicit NNs formulation for mean pressure fluctuation and non-dimensional pressure fluctuation parameter estimations as a function of input parameters. Input parameters and weights of the trained NN were extracted to form an explicit expression in the following manner.

Each input was multiplied by a connection weight and then biases were simply added to this multiplication (Equation 5.1) and finally, the sum was transformed through a transfer function (sigmoid) (Equation 6.2) to generate an output.

In order to acquire accurate results from the ENNF, prior to the execution of the training process of the NN, input and output parameters were normalized in the range of (-0.95; 0.95) by

$$\Gamma_{normalized} = c\Gamma + d \tag{6.4}$$

where Γ represents parameters used in the NN training process, c and d are normalization coefficients of that particular parameter. The dimensional parameters in charge are, $\sqrt{\overline{p'^2}}$, mean pressure fluctuation, y_1, gate opening, u_1, upstream velocity of water issuing from the gate, y_t, tail water depth, x, the distance from the gate to pressure fluctuation measuring point, and the correspondent non-dimensional parameters are $C_p^{'}$, F_1, y_t/y_1 and x/y_1. Taking these parameters into account, $\sqrt{\overline{p'^2}}$ can be functionally expressed as:

$$\sqrt{\overline{p'^2}} = f(u_1, y_1, y_t, x) \tag{6.5}$$

$$\sqrt{\overline{p'^2}} = \left(\frac{100000}{1+e^{-2W}} - 5000\right) \tag{6.6}$$

where

$$\begin{aligned} W = {} & 26.94\left(\frac{1}{1+e^{-2U1}}\right) + 26.30\left(\frac{1}{1+e^{-2U2}}\right) + 38.56\left(\frac{1}{1+e^{-2U3}}\right) - 0.42\left(\frac{1}{1+e^{-2U4}}\right) + 3.32\left(\frac{1}{1+e^{-2U5}}\right) \\ & + 0.54\left(\frac{1}{1+e^{2-U6}}\right) + 27.66\left(\frac{1}{1+e^{-2U7}}\right) - 39.32\left(\frac{1}{1+e^{-2U8}}\right) - 0.30\left(\frac{1}{1+e^{-2U9}}\right) + 3.22\left(\frac{1}{1+e^{-2U10}}\right) \\ & - 2.34)\left(\frac{1}{1+e^{-2U11}}\right) + 0.12\left(\frac{1}{1+e^{-2U12}}\right) + 3.24\left(\frac{1}{1+e^{-2U13}}\right) - 0.04\left(\frac{1}{1+e^{-2U14}}\right) - 26.28\left(\frac{1}{1+e^{-2U15}}\right) \\ & - 0.20)\left(\frac{1}{1+e^{-2U16}}\right) - 31.51 \end{aligned} \tag{6.7}$$

and the values for Ui are given as

$$U1 = (0.91 * u_1) + (0.37 * y_1) + (-1.87 * y_t) + (0.24 * x) + (-35.55)$$

$$U2 = (-1.51 * u_1) + (-0.74 * y_1) + (0.20 * y_t) + (-0.24 * x) + (57.18)$$

$$U3 = (-0.20 * u_1) + (0.06 * y_1) + (-3.15 * y_t) + (0.03 * x) + (13.82)$$

$$U4 = (-1.20 * u_1) + (-1.62 * y_1) + (-1.63 * y_t) + (-0.19 * x) + (87.11)$$

$$U5 = (0.45 * u_1) + (-0.36 * y_1) + (0.98 * y_t) + (0.37 * x) + (-33.45)$$

$$U6 = (-2.17 * u_1) + (-1.74 * y_1) + (7.52 * y_t) + (-0.34 * x) + (81.15)$$

$$U7 = (-0.82 * u_1) + (-0.52 * y_1) + (2.73 * y_t) + (-0.24 * x) + (32.32)$$

$$U8 = (-0.27 * u_1) + (0.21 * y_1) + (-3.57 * y_t) + (0.02 * x) + (15.42)$$

$$U9 = (-5.22 * u_1) + (-2.13 * y_1) + (8.10 * y_t) + (-0.13 * x) + (140.70)$$

$$U10 = (0.28 * u_1) + (0.18 * y_1) + (-0.50 * y_t) + (0.27 * x) + (-31.72)$$

$$U11 = (1.18 * u_1) + (-0.13 * y_1) + (-8.49 * y_t) + (1.00 * x) + (-67.67)$$

$$U12 = (-6.50 * u_1) + (-3.50 * y_1) + (0.78 * y_t) + (-1.14 * x) + (232.17)$$

$$U13 = (-0.76 * u_1) + (-0.04 y_1) + (-1.06 * y_t) + (-0.72 * x) + (87.70)$$

$$U14 = (-1.32 * u_1) + (0.20 * y_1) + (-1.47 * y_t) + (0.04 * x) + (3.00)$$

$$U15 = (-1.40 * u_1) + (-0.90 * y_1) + (1.09 * y_t) + (-0.24 * x) + (54.45)$$

$$U16 = (0.51 * u_1) + (1.49 * y_1) + (-1.42 * y_t) + (-0.03 * x) + (-1.06)$$

and, $C_p^{'}$ can be expressed as:

$$C_p^{'} = f\left(\frac{1}{F_1}, \frac{y_t}{y_1}, \frac{x}{y_1}\right) \tag{6.8}$$

$$C_p^{'} = \left(\frac{0.311}{1 + e^{-2W}} - 0.006\right) \tag{6.9}$$

where

$$W = 11.22\left(\frac{1}{1+e^{-2U1}}\right) - 1.09\left(\frac{1}{1+e^{-2U2}}\right) + 164.19\left(\frac{1}{1+e^{-2U3}}\right) + 6.81\left(\frac{1}{1+e^{-2U4}}\right) + 243.72\left(\frac{1}{1+e^{-2U5}}\right)$$
$$- 1.88) * \left(\frac{1}{1+e^{-2U6}}\right) + 1.34\left(\frac{1}{1+e^{-2U7}}\right) - 3.020\left(\frac{1}{1+e^{-2U8}}\right) + 2.00\left(\frac{1}{1+e^{-2U9}}\right) - 5.77\left(\frac{1}{1+e^{-2U10}}\right) \quad (6.10)$$
$$+ 2.46)\left(\frac{1}{1+e^{-2U11}}\right) - 1.39\left(\frac{1}{1+e^{-2U12}}\right) + 6.90\left(\frac{1}{1+e^{-2U13}}\right) + 79.70\left(\frac{1}{1+e^{-2U14}}\right) - 1.60\left(\frac{1}{1+e^{-2U15}}\right)$$
$$+ 1.48\left(\frac{1}{1+e^{-2U16}}\right) + 0.33\left(\frac{1}{1+e^{-2U16}}\right) - 248.08$$

and the values for Ui are given as

$$U1 = (119.21*1/F_1) + (-0.16*y_t/y_1) + (-0.03*x/y_1) + (-1.98)$$

$$U2 = (89.52*1/F_1) + (1.81*y_t/y_1) + (-0.19*x/y_1) + (-14.75)$$

$$U3 = (23.70*1/F_1) + (0.52*y_t/y_1) + (-0.02*x/y_1) + (-4.72)$$

$$U4 = (1183.75*1/F_1) + (-3.46*y_t/y_1) + (2.68*x/y_1) + (-77.78)$$

$$U5 = (-18.83*1/F_1) + (-0.45*y_t/y_1) + (0.02*x/y_1) + (3.77)$$

$$U6 = (95.10*1/F_1) + (*y_t/y_1) + (0.22*x/y_1) + (-8.76)$$

$$U7 = (277.02*1/F_1) + (0.10*y_t/y_1) + (0.52*x/y_1) + (-8.83)$$

$$U8 = (927.57*1/F_1) + (-14.42*y_t/y_1) + (0.25*x/y_1) + (92.46)$$

$$U9 = (315.72*1/F_1) + (-0.43*y_t/y_1) + (-0.15*x/y_1) + (1.08)$$

$$U10 = (-165.04*1/F_1) + (0.85*y_t/y_1) + (0.04*x/y_1) + (1.45)$$

$$U11 = (216.60*1/F_1) + (1.81*y_t/y_1) + (0.21*x/y_1) + (-24.97)$$

$$U12 = (555.19*1/F_1) + (-1.85*y_t/y_1) + (-0.40*x/y_1) + (11.70)$$

$$U13 = (-803.30*1/F_1) + (3.66*y_t/y_1) + (-2.30*x/y_1) + (55.57)$$

$$U14 = (10.98*1/F_1) + (0.65*y_t/y_1) + (-0.02*x/y_1) + (-4.33)$$

$$U15 = (151.39 * 1/F_1) + (2.07 * y_t / y_1) + (0.28 * x / y_1) + (-26.39)$$

$$U16 = (-51.50 * 1/F_1) + (-0.44 * y_t / y_1) + (0.26 * x / y_1) + (-1.46)$$

$$U17 = (477.74 * 1/F_1) + (0.18 * y_t / y_1) + (0.34 * x / y_1) + (-22.79)$$

It should be noted that ENNF in Equations (6.6) and (6.9) are valid for parameters ranging between the maximum and minimum values given in Tables 4.1 and 4.2, respectively

6.5 Prediction of pressure fluctuation using regression analysis

Nonlinear regression analysis was applied for characterization of the complex mapping among considered parameters. In this context nonlinear relations were developed between non-dimensional pressure fluctuation, $C_p^{'}$ and the non-dimensional input parameters. Among the derived regression equations, the most efficient ten are presented in Table 6.3. The coefficients of the regression models were calculated by Genetic Algorithm, using commercial software.

6.6 Results of regression analysis

Resulting regression coefficients (*pi*) are given in Table 6.4. Referring to the statistical results,nonlinear regression models produced slightly good outcomes, namely identification of target mapping with nonlinear behaviours produced good results in terms of correlation coefficient (*R*) and root mean square errors (RMSE). In this sense, Model 2 (*R*= 0.69) and Model 8 (*R*=0.67) were selected to be representative nonlinear models. Statistical parameters of regression models are given in Table 6.5.

In order to evaluate the relative performances of nonlinear regression models, scatter plots (Figures 6.7-6.8) of Model 2 and Model 8 are illustrated. As can be seen from Figures 6.7 and 6.8, discrepancies from best fit line in nonlinear Model 2 are slight smaller than nonlinear Model 8. It can be concluded that nonlinear analysis exhibited good performance in predicting nondimensional pressure fluctuation parameter.

6.7 Neural network modelling versus regression analysis

The overall performances of neural network modelling and regression analysis are compared through R and RMSE values of each model. Predictions of NN Model 2 to observed ones (given in Figure 6.6, R= 0,988, RMSE= 0,0012) are considerably better than the regression models 2 and 8 (Figures 6.7and 6.8, R=0,690, RMSE=0,0015 and R= 0,670, RMSE= 0,0020, respectively). It can be concluded that neural network modelling exhibited coniderable dominance over regression analysis in predicting the mean pressure fluctuation beneath hydraulic jump.

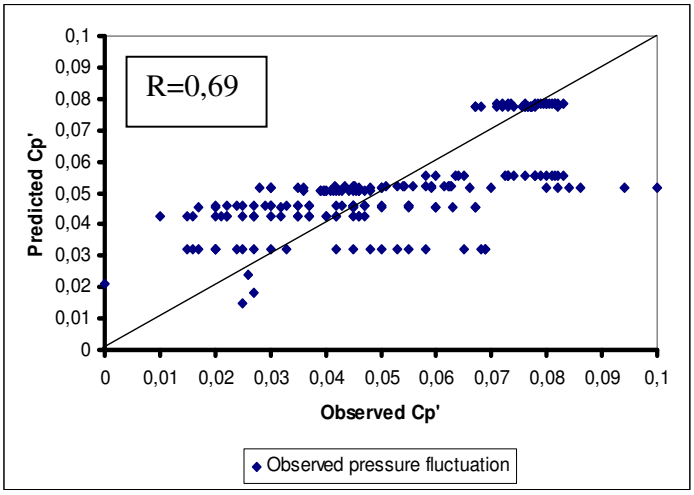

Figure 6.7 Prediction of nonlinear regression Model 2 and observed values

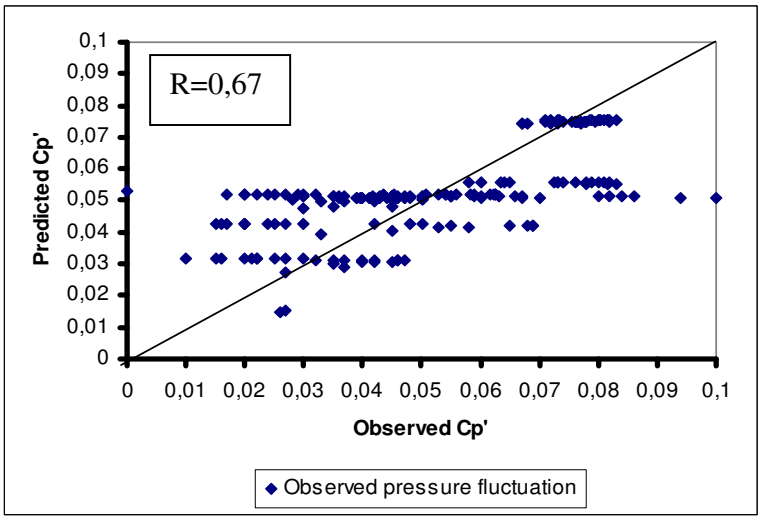

Figure 6.8. Prediction of nonlinear regression Model 8 and observed values

Table 6.3. Proposed nonlinear models

NONLINEAR MULTIPLE REGRESSION MODEL	
MODEL NO	*MODEL FUNCTIONS*
1	$y = p1*(1/F_1\text{^}p2+y_t/y_1\text{^}p3+x/y_1\text{^}p4)+p5$
2	$y = p1+p2*(1/(p3+p4*1/F_1)+1/(p5+p6*\ y_t/y_1)+1/(p7+p8*\ x/y_1))$
3	$y = p1+p2*(\exp(p3+p4*1/F_1)+\exp(p5+p6*\ y_t/y_1)+\exp(p7+p8*\ x/y_1))$
4	$y = p1+p2*(\exp(-p3*1/F_1)+\exp(-p4*\ y_t/y_1)+\exp(-p5*\ x/y_1))$
5	$y = p1+p2*(\exp(p3*1/F_1)+\exp(p4*\ y_t/y_1)+\exp(p5*\ x/y_1)$
6	$y = p1+p2*(1/F_1+\ y_t/y_1+\ x/y_1)+p3*(1/F_1\text{^}2+\ y_t/y_1\text{^}2+\ x/y_1\text{^}2)+\ p4*\ (1/F_1\text{^}3+\ y_t/y_1\text{^}3+\ x/y_1\text{^}3)\ +p5*(1/F_1\text{^}4+\ y_t/y_1\text{^}4+\ x/y_1\text{^}4)+p6*(x1\text{^}5+\ y_t/y_1\text{^}5+\ x/y_1\text{^}5)$
7	$y = p1+p2*(1/F_1\text{^}p3+\ y_t/y_1\text{^}p4+\ x/y_1\text{^}p5);$
8	$y = p1+p2*(1/(p3+p4*1/F_1)+1/(p5+p6*\ y_t/y_1)+1/(p7+p8*\ x/y_1))$
9	$y = p1+p2*\exp((p3/1/F_1)+(p4/\ y_t/y_1)+(p5/\ x/y_1));$
10	$y = p1+p2*(1/(1/F_1)+1/\ y_t/y_1+1/\ x/y_1)+p3*\exp(1/1/F_1+1/\ y_t/y_1+1/\ x/y_1)+\ p4*\ln(1/1/F_1+1/\ y_t/y_1+1/\ x/y_1)$

Table 6.4 Model coefficients of proposed nonlinear regression models

MODEL NO	*p1*	*p2*	*p3*	*p4*	*p5*	*p6*	*p7*	*p8*
1	-4,924	0,291	-0,506	2,185	0,056			
2	0,050	-1,438	0,053	-1,316	0,002	-0,001	5,188	7641,2
3	0,088	-0,003	-48,187	1065,96	3,438	-0,284	1,702	0,027
4	0,244	-0,082	-2,666	0,284	-0,008			
5	0,244	-0,082	-2,666	0,284	-0,008			
6	-0,013	0,008	-0,001	4,463	1,443	-2,283		
7	0,056	-4,924	0,291	-0,506	2,185			
8	0,048	0,073	20,849	-635,73	49,137	-7,206	-1,973	-13,140
9	0,035	266130	-0,141	-84,492	-0,180			
10	-0,122	-0,001	-7,518	0,063				

Table 6.5. Statistical results of proposed nonlinear regression models

MODEL NO	*RMSE*	*SSE*	*R*
1	0,019845808	0,07562037	0,308162643
2	0,015051604	0,04349775	0,692396199
3	0,018137225	0,06316011	0,494055097
4	0,019007157	0,06936423	0,412114872
5	0,019007157	0,06936423	0,412114872
6	0,017147038	0,05645202	0,569538346
7	0,019845808	0,07562037	0,308162644
8	0,015469675	0,04594768	0,67088846
9	0,016844593	0,05447814	0,594401952
10	0,01961366	0,07386157	0,356629663

CHAPTER 7

CONCLUSISONS AND FUTURE STUDIES

7.1 Conclusions

(1) Two neural network models with sizes of 4-16-1 and 3-17-1 are found to be optimum with hyperbolic tangent sigmoid transfer function (tansig).

(2) Explicit formulations that predict mean pressure fluctuation and the non-dimensional pressure fluctuation parameter, in terms of the most contributing variables of hydraulic jump occurring on stilling basins, are presented.

(3) Artificial Neural Networks are found to be successively capable of modelling the pressure fluctuations beneath hydraulic jumps occurring on horizontal stilling basins.

(4) It is observed that there is a good agreement between the predicted results and the measured values and they are close to the line of the perfect agreement due to relatively small values of the error (MAPE).

(5) ANNs can be used as an effective tool to establish the correlation among physical variables and they have a generalised potential to represent input and output relationships.

(6) Nonlinear regression analysis on exprimental data revealed a number of nonlinear equations. The performances of regression equations are compared with those of

neural networks. Predictions of NNs are found to be clearly better than those of non-linear regression equations.

7.2 Future Studies

(1) Additional experimental and field data may be used in order to improve the generalization capacity of the proposed models.

(2) The slope of inclined sill should be considered as an effective parameter influencing the case and some other physical parameters can be considered as input.

(3) Other artifical intelligenece techniques such as Genetic Programming, Fuzzy Logic and Neuro-fuzzy can be used to capture the highly nonlinear and complex nature of the problem.

REFERENCES

1. Abdul Khader, M. H., and Elango, K. (1974). Turbulent pressure field beneath a hydraulic jump. *J. Hydr. Res*., IAHR, 12(4), 469-489.
2. Akbari, M. E., Mittal, M. K., and Pande, P. K. (1982). "Pressure fluctuations on the floor of free and forced hydraulic jumps." *Proc. Int. Conf. On the Hydraulic Modeling of civil Eng. Struc*., BHRA Fluid ENGRG., Coventry, England, paper C1, pp 87-96.
3. Azmathullah H. Md., Deo M. C., and Deolalikar, P. B. (2005). Estimation of scour below spillways using neural networks. *J. of Hydraulic Research*., IAHR, 44(1), 61-69.
4. Baxter C.W., Zhang, Q. S., Stanley, J. R., Shariff, R., Tupas, R.T., and Stark, H.L. (2001). Drinking water quality and treatment: the use of artificial neural networks. *Can. J. of Civ. Eng*., 28(S1), 26-35.
5. Bishop, C. (1995). Neural Networks for Pattern Recognition, Oxford.
6. Bowers, C.E., Tsai, F.Y., and Kuha, R.M. (1964). Hydraulic studies of the spillway of Karnafuli hydroelectric project, East Pakistan. Project Report No. 73, St. Anthony Falls Hydraulic Lab., Univ. of Minnesota, Minneapolis, Minn., pp 1-380.
7. Çevik, A. (2006). " A new approach for elastoplastic analysis of structures: neural networks". PhD Thesis, University of Gaziantep.
8. Dolling, R.O., and Varas, E.A. (2002). Artificial neural network for stream flow prediction. *J. of Hydr. Res*., IAHR, 4(5), 547-554.
9. Elder, Rex A. (1961). "Model-Prototype turbulence scaling." *Proc., Ninth Convention of IAHR,* Dobrovnik, Yogoslavia, pp 24-31.

10. Gunal, M. (1996). *Numerical and experimental investiagation of hydraulic jumps*. Ph.D. Thesis Submitted to University of Manchester Institute of Science and Technology, Manchester, UK.
11. Fattor, C.A., Lopardo, M.C., Casado, J.M, and Lopardo R.A. (2001). Cavitation by macro-turbulent pressure fluctuations in hydraulic jump stilling basins. *Proc. of 29th IAHR Congress*, Sept., 16-21, Beijing, China.
12. Fiorotto, V., and Rinaldo, A. (1992). Fluctuating uplift and lining design in spillway stilling basins. *J. of Hydr. Eng*., ASCE, 118(4): 578-597.
13. Flood, I. (1989). A Neural Network approach to the sequencing of construction tasks. *Proc. of 6th Conf. of SARC*, San Francisco, USA.
14. Hager, W.H. (1989). B-jump in sloping channel. *J. of Hydr. Res*., IAHR, 27(1), 539-558.
15. Haykin, S. (2000). *Neural Networks- A Comprehensive Foundation*. Macmillan College Publications Cooperation.
16. Hebb, D.O. (1949). *The Organization of Behaviour*. Wiley, New York.
17. Grubert, J. P. (1995). Application of Neural Networks in Stratified Flow Stability Analysis. *J. of Hydr. Eng*., 121(7), 523-532.
18. Kambekar, A. R. and Deo, M. C. (2003). "Estimation of pile group scour using neural networks" *J. of Applied Ocean Research,* 25(4), 225-234.
19. Karunanuthi, N., Grenney, W.J., Whitley, D., and Bovee, K. (1994). Neural Networks for river flows prediction. *J. of Computing in Civ. Eng*., ASCE, 8(2), 201-219.

20. Kavianpour M.R. (2000). Statistical characteristics of pressure fluctuations downstream of deflectors. *8th International Symposium on Stochastic Hydraulics*, Beijing, China.
21. Levitt, R.E., Kartam, N.A., Kunz, J.C. (1988). Artificial intelligence techniques for generating construction project plans. *J. of Construction Eng. and Management*, ASCE, 114(3), 329-343.
22. Leutheusser, H. J., and Kartha, V. C. (1972) "Effect of inflow condition on the hydraulic jump." *J. Hydr. Div*., ASCE, 98 (HY8),1367-1386.
23. Liu, W., and James, C.S. (2000). Estimation of discharge capacity in meandering compound channels using neural networks. *Canadian Journal of Civil Engineerin*g, 27, 297-308.
24. Lopardo, R.A., and Henning, R.E. (1985). Experimental advances on pressure fluctuations beneath hydraulic jumps. *Proc. of the 21st IAHR Congress*, Melbourne, Australia, 3, 633-638.
25. Lopardo, R.A., Fattor, C.A., Lopardo, M.C. and Casado, J.M. (2004). *Instantaneous pressure field on a submerged jump stilling basin. Hydraulics of Dams & River Structures* , A.A. Balkema Publishers, Editors Farhad Yazdandoost and Jalal Attari, London, U.K., ISBN 90 5809 673 4, Part I, pp 133-138.
26. Lopardo, R.A., De Lio, J.C., and Lopardo, M.C. (1999). Physical modelling and design estimation of instantaneous pressures in stilling basins. *Proc. of the 28th IAHR Congress*, Graz.
27. Maier, H.R. and Dandy, G.C. (2000). Neural Networks for prediction and forecasting of water resources variables; a review of modelling issues and applications. *Environmental Modelling and Software* (Elsevier), 15, 101-124.

28. Minsky, M., and Pappert, S. (1969). *Perceptrons*. MIT Press, Cam-bridge, MA.

29. Nagy, H. M., Watanabe, K., and Hirano M. 2002. Prediction of sediment load concentration in rivers using Artificial Neural Network model. *J. of Hydr. Eng*., ASCE, 128(6), 588-595.

30. Narasimhan, S., and Bhargava, V.P. (1976). Pressure fluctuations in submerged jump. *Proc. of ASCE, J. of Hydr. Division*, ASCE, 102(HY3), 1331-1342.

31. Narayanan, R. (1978). Pressure fluctuations beneath submerged jump. *Proc. of ASCE, J. of Hydr. Division*, ASCE, 106(HY4), 339-350.

32. Negm A.M. (2001). Prediction of hydraulic design parameters of expanding stilling basins using Artificial Neural Network. Egyptian *Journal for Engineering Science and Technology* (EJEST), Faculty of Engineering, Zagazig University, Egypt.

33. Negm, A.M., and Shouman, M.A. (2002). Artificial Neural Network model for submerged hydraulic jump over roughened floor. *Proc. of the 2nd Int. Conf. for Advanced Trends in Engineering*, April 7-9, El-Minia Univ., El-Minia, Eqypt.

34. Ohtsu, I., and Yasuda, Y. (1990). B-jump in sloping channel. *J. of Hydr. Res*., IAHR, 28(1), 105-119.

35. Ohtsu, I., and Yasuda, Y. (1991). Hydraulic jump in sloping channels. *J. of Hydr. Eng*., ASCE, 117(7), 905-921.

36. Pirooz B. and Kavianpour M. R. (2005). "Experimental investigation of pressure fluctuations beneath hydraulic jump." *Proceeding of the 29th IAHR Congress*, Septemver 2001, Beijing, China.

37. Rinaldo, A. and Fiorotto, V. (1993). " Turbulent pressure fluctuations under hydraulic jumps." *Journal of hydraulic research*, 30(4), 499-520

38. Rouse, H., Sio, t. t. and Nagaratnam, s. (1959). " Turbulence characteristics of the hydraulic jump." *Trans. ASCE*,124,926-950.

39. Rumelhart, D.E., Hinton, G.E., and Williams, R.J. (1986). *Learning internal representation by error propagation Parallel Distributed Processing: Exploration in the Microstructure of Cognition*. Vol. 1, Chapter 8, MIT Press, Cambridge, MA.

40. Sarghini, F., de Felice, G., and Santini, S. (2003). Neural Networks based subgrid scale modelling in large eddy simulations. *J. of Computers and Fluids*, 32,(1): 97-108.

41. Schiebe, F., and Bowers, C. E. (1971). " Boundary pressure fluctuations due to macroturbulence in hydraulic jumps." *Proc. Symp. On Turbulence in liquids,* Univ. of Missouri, Columbia, Mo.

42. The ASCE Task Committee. (2000). The ASCE Task Committee on application of the Neural Networks in hydrology. *Journal of Hydraulic Engineering*, 5(2): 115-137.

43. Toso, J., and Bowers, E.C. (1988). Extreme pressures in hydraulic jump stilling basin. *J. of Hydr. Eng*., ASCE, 114(8), 829-843.

44. Vasiliev, O. F., and Bukreyev, V. I. (1967). Statistical Characteristics of pressure Fluctuations in the region of hydraulic jump. *Proc., 12th Congress International Associations of Hydraulic Research*, 2: 1-8.

45. Zupan, J., and Gasteiger, J. (1993). *Neural Networks for Chemists - An Introduction*. VCH,Weinheim.